© American Society for Mass Spectrometry, 2014

J. Am. Soc. Mass Spectrom. (2014)
DOI: 10.1007/s13361-013-0813-8

RESEARCH ARTICLE

LC-MS/MS Analysis and Comparison of Oxidative Damages on Peptides Induced by Pathogen Reduction Technologies for Platelets

Michel Prudent, Giona Sonego, Mélanie Abonnenc, Jean-Daniel Tissot, Niels Lion

Service Régional Vaudois de Transfusion Sanguine, Unité de Recherche et Développement, Lausanne, Switzerland

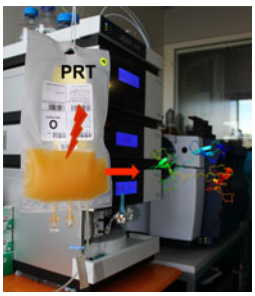

Abstract. Pathogen reduction technologies (PRT) are photochemical processes that use a combination of photosensitizers and UV-light to inactivate pathogens in platelet concentrates (PCs), a blood-derived product used to prevent hemorrhage. However, different studies have questioned the impact of PRT on platelet function and transfusion efficacy, and several proteomic analyses revealed possible oxidative damages to proteins. The present work focused on the oxidative damages produced by the two main PRT on peptides. Model peptides containing residues prone to oxidation (tyrosine, histidine, tryptophane, and cysteine) were irradiated with a combination of amotosalen/UVA (Intercept process) or riboflavin/UVB (Mirasol-like process). Modifications were identified and quantified by liquid chromatography coupled to tandem mass spectrometry. Cysteine-containing peptides formed disulfide bridges (R-SS-R, –2 Da; favored following amotosalen/UVA), sulfenic and sulfonic acids (R-SOH, +16 Da, R-SO_3H, +48 Da, favored following riboflavin/UVB) upon treatment and the other amino acids exhibited different oxidations revealed by mass shifts from +4 to +34 Da involving different mechanisms; no photoadducts were detected. These amino acids were not equally affected by the PRT and the combination riboflavin/UVB generated more oxidation than amotosalen/UVA. This work identifies the different types and sites of peptide oxidations under the photochemical treatments and demonstrates that the two PRT may behave differently. The potential impact on proteins and platelet functions may thus be PRT-dependent.

Key words: Amotosalen, Mass spectrometry, Oxidation, Peptide, Platelet, Riboflavin

Received: 27 September 2013/Revised: 21 November 2013/Accepted: 13 December 2013

Introduction

Platelet concentrates (PCs) are one of the blood products used in transfusion medicine and are given to stop hemorrhage in patients with low level of platelets or to prevent hemorrhage after a cancer patient has had chemotherapy. PCs are stored in additive solution or plasma at room temperature under agitation up to 5 d (7 d if secured by a step of pathogen reduction). Pathogen reduction technologies (PRT) for PC are in routine use in several countries worldwide with the aim of rendering platelet transfusions safer towards transfusion-transmitted infections. Intercept Blood System for PC (Cerus Europe BV) [1] and Mirasol PRT (Terumo BCT Biotechnologies) [2] are now in use in 21 and 18 countries, respectively [3]. Even though PRT have shown their efficacy, different in vitro and clinical studies have reported the impact of PRT on platelet function and transfusion efficacy. The MIRACLE trial on Mirasol reported a slightly lower corrected count increment (CCI, which represents the level of platelets in patients 1 or 24 h after the transfusion, in other words the efficacy of transfusion) with treated PC with no concomitant increase in blood product consumption [4]. Clinical trials on Intercept have also reported the decrease in CCI, but these studies are under debate showing the difficulty in comparing the dataset [5–12]. In vitro experiments have also been carried out on Intercept- [13, 14] and Mirasol-treated PC [15–17]. Some of those reported an impact of PRT on agonist-induced aggregation, glycoprotein expression, p-selectin expression, and annexin V binding, whereas others did not, as shown for example by Hechler et al., where similar data were obtained in both treated and untreated PC [14]. More recently, several papers were published on proteomic analyses of treated

Michel Prudent and Giona Sonego contributed equally to this work.

Electronic supplementary material The online version of this article (doi:10.1007/s13361-013-0813-8) contains supplementary material, which is available to authorized users.

Correspondence to: Niels Lion; *e-mail:* niels.lion@mavietonsang.ch

Published online: 28 January 2014

platelets [14, 18–24]. They pointed out the relatively low impact on the proteome of treated platelets (independently of storage lesions) and some data show that the treatment leads to an acceleration of storage lesion. Proteins involved in platelet metabolism, activation and aggregation, cytoskeleton organization, signal transduction, and oxidative stress were impacted by these treatments. In particular, it has been reported by our laboratory that the Intercept process affects DJ-1 and glutaredoxin-5, proteins related to oxidative stress defenses [19].

Intercept and Mirasol processes are based on the photochemical modifications of DNA and RNA strands, thus preventing pathogen replication. Nevertheless, the two processes are slightly different. Intercept uses an intercalator, amotosalen, which primarily cross-links strands upon UVA irradiation [25, 26] and generates reactive oxygen species (ROS) [27, 28]. Following the absorption of a photon, the excited amotosalen reacts with one strand through a [2 + 2] photocycloaddition that forms a 5,6-double bound on a thymine [27, 28]. After the absorption of a second photon by the furan-side, the amotosalen can bind to the other DNA strand. The reaction is also feasible on uracil bases but is 6 to 8 times slower than with DNA [28, 29]. On the other hand, Mirasol employs riboflavin as a photosensitizer that does not dock to DNA/RNA strands but generates ROS. Its excited state oxidizes preferentially purine bases (mainly guanine residues) by direct electron transfer [30]. The reaction is irreversible and alters the replication of pathogen.

Amotosalen and riboflavin are photosensitizers able to directly oxidize other molecules and to generate ROS. Photochemical reactions can be classified in two categories, type I and type II mechanisms (see Scheme 1) [28, 30], and both amotosalen and riboflavin can be involved in these two mechanisms. The former involves electron transfer to triplet oxygen ($^3O_2$) after the oxidation of a substrate (S). It leads to the formation of superoxide anions ($O_2^{\bullet -}$). The latter involves energy transfer to $^3O_2$ that leads to the formation of singlet oxygen (an excited state of oxygen, $^1O_2$).

Although the primary targets of the photosensitizers in PC are nucleic acids, the presence of radical cations and ROS can also damage other compounds such as proteins. Amino acids can be oxidized by the two types of mechanisms. The main targets are sulfur-containing amino acids, i.e., cysteine (Cys) and methionine (Met), and histidine (His), tryptophan (Trp) and tyrosine (Tyr) [31]. The rate of quenching of $^1O_2$ depends on residues and is as follows: His>Trp>Met>Tyr>Cys [32, 33]. In the case of cysteine, the oxidation leads to the formation of disulfide bridges (if the concentration is high enough) and sulfenic, sulfinic, and sulfonic acids. Depending on the conditions, riboflavin oxidizes these amino acids following a type I and/or type II reactions [32]. Indeed, amino acids react with excited riboflavin with similar rates, and type I reactions will be favored in absence of oxygen. As riboflavin, the psoralen-derivative amotosalen also induces these oxidations [27]. Amino acids are oxidized by 8-methoxypsoralen (8MOP) radical cations as follows: Tyr>Trp>Cys>His>Met [34]. Moreover, Sastry reported that psoralen-derivatives can directly react with proteins to form a photoadduct on Tyr residues [35]. These photoadducts were also demonstrated by Schmitt et al., even though the amount was very low (a few adducts/thousands of amino acids) [36].

In the present article, the effects of the PRT, amotosalen/UVA, and riboflavin/UVB were evaluated on model peptides that contain cysteine, tryptophan, histidine, or tyrosine amino acids (see Table 1). Peptides were chosen in order to probe the different types of residues prone to oxidation, and the potential formation of photoadducts. The types of modifications and damages induced by the treatments were determined and quantified by liquid chromatography coupled to tandem mass spectrometry (LC-MS/MS) in order to highlight the potential differences between the PRT.

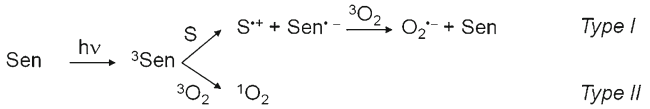

Scheme 1. Photochemical processes, type I and type II. Sen=photosensitizer, S=substrate. $^3O_2$: ground state oxygen, $^1O_2$: singlet oxygen

Experimental

Chemicals

Amotosalen-HCl 3 mM (3-[(2-aminoethoxy)methyl]-2,5,9-trimethyl-7*H*-furo[3,2-*g*][1]benzopyran-7-one hydrochloride, *M* = 337.8 g/mol) and InterSol additive solutions (15 mM sodium citrate, 21 mM disodium phosphate, 7 mM sodium phosphate dihydrate, 54 mM sodium acetate, and 77 mM sodium chloride) were taken from the Intercept Blood System kit used for the pathogen inactivation in PC provided by Cerus Europe BV (Amersfoort, The Netherlands). The InterSol additive solution was from Fenwal (Lake Zurich, IL, USA). Riboflavin (>98 %) from Sigma-Aldrich (Steinheim, Germany), was prepared in stock solution at 1 g/L in 0.9 % NaCl and stored in the dark at –28 °C. Peptides (see Table 1): cC (AAACAAA, *M* = 547.6 g/mol), cH (AAAHAAA,

Table 1. List of Peptides (Potential Targets are in Bold)

Peptide	Sequence	*m/z* (M + H$^+$)	*MW* (g/mol)
cC	AAA**C**AAA	548.2	547.6
cH	AAA**H**AAA	582.3	581.7
cW	AAA**W**AAA	631.2	630.7
YY	**YY**	345.1	344.1
M	RG**Y**LAG	636.2	635.7
angII	DRV**YI**H**P**F	523.2 (*z* = 2)	1,046.2
Fib seq	**C**QDSETRTF**Y**	625.7 (*z* = 2)	1,249.3

M = 581.7 g/mol), cW (AAAWAAA, M = 630.7 g/mol), dityrosine (YY, M = 344.1 g/mol), M (RGYLAG, M = 635.7 g/mol), angiotensin II (angII, DRVYIHPF, M = 1,046.2 g/mol), and fibronectin sequence (Fib seq, CQDSETRTFY, M = 1,249.3 g/mol) were bought from Bachem (Bubendorf, Switzerland). Deionized water (>15 MΩ·cm) was prepared using an ELGA OPTION 4 apparatus (Omnilab AG, Mettmenstetten, Switzerland). Acetonitrile (ACN, >99.9 %) gradient grade for HPLC was purchased from Sigma-Aldrich (Steinheim, Germany), and trifluoroacetic acid (TFA, 99.0 %) and formic acid (FA, 98.0 %) from Fluka (Steinheim, Germany).

The synthetic peptides were customized in order to test the reactivity of one amino acid at a time and to avoid cyclization (for cH and cW) (e.g., between NH_3 terminus and aromatic ring). The dityrosine peptide was chosen to probe the potential formation of intra- and inter-crosslinks, angII because it contains two potential targets and the fibronectin sequence because it represents an active domain of fibronectin involved in thrombus formation [37].

Sample Preparation

A solution of 20 µL containing the peptide at 50 µM (from stock solution of 1 g/L in H_2O) and the photoactive molecule at 100 µM (amotosalen or riboflavin) were prepared in InterSol (compatible for both Intercept and Mirasol system). As controls (peptide alone, peptide+UV), solutions of peptides at 50 µM were also prepared in InterSol medium. Samples (in triplicate) were prepared fresh daily and kept at 4 °C in the dark before UV irradiation or LC-MS/MS analysis.

Amotosalen/UVA Treatment UV irradiations were performed under the same conditions used in routine for the pathogen inactivation with Intercept Blood System [1]. Samples were placed in 1.5-mL tubes (polypropylene tubes, Eppendorf AG, Hamburg, Germany), were put inside the illuminator (INT100; Cerus Europe BV, Amersfoort, The Netherlands) and were treated with one dose (3.9 J/cm^2, approximately 3.5 min) of UVA at 22 °C under agitation.

Riboflavin/UVB Treatment In Switzerland, the Incerpt process is exclusively used as PRT. Thus, a homemade setup was built for riboflavin/UVB treatment, in order to reproduce the Mirasol process and to provide 5 J/cm^2, necessary to convert 21.1 % of riboflavin [38]. Samples were put inside a dark cabinet and were illuminated from top and bottom (100 mm) with 2 × 4 UVB lamps (Philips UVB Broadband TL 100 W/12; Elevite, Switzerland; see UV spectrum in Figure S1 in Supporting Information) during 12.5 min at 22 °C under agitation. The dose delivered was measured with a UVX radiometer (UVX-31 from UVP, Cambridge, UK). The temperature inside the illumination cabinet was monitored with a thermometer (Ecolog TP4-L; ELPRO, Buchs, Switzerland).

LC-MS/MS Analyses

Samples and products of reactions were analyzed using an HPLC coupled to an ESI-MS (UHPLC focused Thermo Scientific Dionex UltiMate 300 Series; Thermo Scientific, Germering, Germany; and MS amaZon ETD, from Bruker Daltonik, Bremen, Germany). Samples (1 µL) were injected on an Acclaim PepMap reversed phase C-18 column (3.5 µm, 150 × 0.3 mm) from Dionex (Amsterdam, The Netherlands). The mobile phase, excepted for peptide M, consisted of solvents A (H_2O + 0.1 % TFA) and B (ACN/H_2O 6/4 + 0.1 % TFA). The starting condition was 1 % of B. After 5 min, an increase of B from 1 % to 99 % was applied during 25 min, followed by a plateau at 99 % of B for 5 min. Then, the column was re-equilibrated by setting down B at 1 % in 1 min and finally ran during 10 min, for a total run time of 46 min. Because peptide M overlapped with riboflavin, solvents A and B consisted of H_2O + 0.1 % FA and H_2O/ACN 2/8 + 0.08 % FA, respectively, and the gradient profile was as described above but B was set at 5 %. The flow rate was fixed at 4 µL/min and the MS capillary voltage was set at 4.5 kV. Tandem mass spectrometry for the identification of modification sites was run automatically on the three most abundant peaks with an exclusion time of 1.5 min.

Data Treatment

Modifications were identified by MS and the fragments were verified with Biotools (ver. 3.2; Bruker Daltonik, Bremen, Germany). Relative quantitation and peak areas were measured by UV (at 214 nm) with Hystar Post Processing software (Bruker Daltonik, Bremen, Germany). To compare the two inactivation processes, monomers (MH^+) and oxidized species (both disulfide bridges forming dimers, D, and adduct of oxygen atoms, M_{ox}) were considered, and the corresponding areas were collected from three replicates per peptide. The conversion rates were defined as follows [39]:

$$\text{conversion rate}\left(M_{ox,i}\right) = \frac{\mathrm{A}\left(M_{ox,i}\right)}{\mathrm{A}(MH^+) + \mathrm{A}(D) + \sum_{i=1}^{n}\mathrm{A}\left(M_{ox,i}\right)} \cdot 100\% \quad (1)$$

$$\text{conversion rate}\,(D) = \frac{\mathrm{A}(D)}{\mathrm{A}(MH^+) + \mathrm{A}(D) + \sum_{i=1}^{n}\mathrm{A}\left(M_{ox,i}\right)} \cdot 100\% \quad (2)$$

$$\text{conversion rate}\left(M_{totalox}\right) = \frac{\mathrm{A}(D) + \sum_{i=1}^{n}\mathrm{A}\left(M_{ox,i}\right)}{\mathrm{A}(MH^+) + \mathrm{A}(D) + \sum_{i=1}^{n}\mathrm{A}\left(M_{ox,i}\right)} \cdot 100\% \quad (3)$$

where A(x) stands for the absorbance at 214 nm in mAU·s, $M_{ox,i}$ stands for the oxidized peptide i, D for the dimer form, MH^+ for the unreacted peptide and $M_{total\ ox}$ for both types of oxidation. Finally, the data were expressed as the mean +/– the standard deviation of the mean.

T-test analyses were performed between conversion rates of peptides treated with amotosalen/UVA or riboflavin/UVB using the software R ver.3.0.1 (The R Foundation for Statistical Computing). *P* values lower than 0.05 were considered (*$P<0.05$, **$P<0.01$, ***$P<0.001$). It has to be noticed that abundances of $M_{ox,i}$ can vary from one replicate to another one, and that the sums of all $M_{ox,i}$ were considered for data treatment.

Results

The amotosalen/UVA treatment was performed with the commercial Intercept illuminator; Figure 1a and b show the degradation of amotosalen upon UVA irradiation: all major peaks were identified as the amotosalen monomer, dimer, and trimer, and amotosalen without the hydrophilic tail (2-aminoethan-1-ol, T, peaks b1-6, Figure 1b). Under these conditions, the residual amotosalen was 10.5 %±0.8 % ($n = 3$, data not shown), which is equivalent to the degradation reported by Liu et al. (15 %) [40]. In parallel, validation of the homemade riboflavin/UVB setup was required and was performed thanks to riboflavin degradation rate given by Goodrich et al. (21.1 % conversion) [38]. Riboflavin degradation was followed by LC-MS/MS and conversion rates were obtained according to LC data (see Figure S2 in Supporting Information). A kinetic curve was followed up to 90 min of illumination, and a degradation of 21.1 % was reached after 12.5 min of irradiation. The irradiation time for peptide oxidation was thus set at 12.5 min. It has to be pointed out that this treatment induces an increase of 3 °C inside the illumination cabinet (data not shown). Hence, the setup fits with the requirement for riboflavin/UVB system. In addition, formation of formylmethyl flavin (cyclization of the α alcohol of the ribitol chain with the ring moiety), riboflavin, 2'keto-flavin and 4'keto-flavin (oxidation of alcohol 2' respectively 4') and, the major degradation product corresponding to lumichrome (loss of the ribitol moiety) were observed (peaks d1-4, Figure 1d).

Seven peptides were treated with amotosalen/UVA or riboflavin/UVB setup and products were studied by LC-MS/MS. In general, the treatment induced the oxidation of peptides; UV alone (shown as control) or photosensitizer alone (data not shown) does not exhibit more oxidation than the peptide alone (data not shown) under these conditions (see Figure 2a and UV chromatograms in Supporting Information). The modifications were observed and quantified by LC (UV chromatograms of cW are shown in Figure 2 as an example; others are shown in Supporting Information) and they were characterized by MS/MS (as shown in Figure 3 for cW,

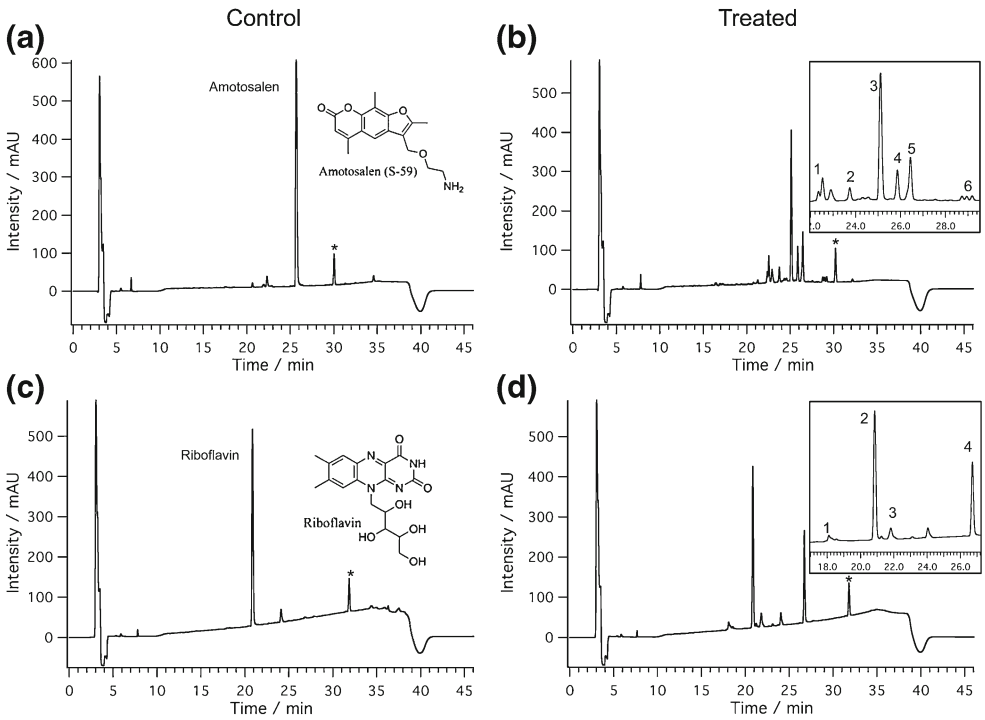

Figure 1. UV chromatograms at 214 nm of the photosensitizers. Amotosalen before (**a**) and after (**b**) UVA treatment. **b1** amotosalen -T (*m/z* 240.3), **b2** dimer (*m/z* 603.2), **b3** amotosalen (*m/z* 301.9), **b4** monomer-T/trimer (*m/z* 240.3/904.4), **b5** dimer-T/trimer (*m/z* 603.2/904.4), **b6** loss of ammonium (*m/z* 284.0). T stands for tail (2-aminoethan-1-ol, $NH_2(CH_2)OH$). Riboflavin before (**c**) and after (**d**) UVB treatment; **d1** formylmethyl flavin (*m/z* 284.1), **d2** riboflavin (*m/z* 377.2), **d3** 2'keto-flavin/4'keto-flavin (*m/z* 375.1), **d4** lumichrome (*m/z* 242.4). *Contaminant coming from InterSol

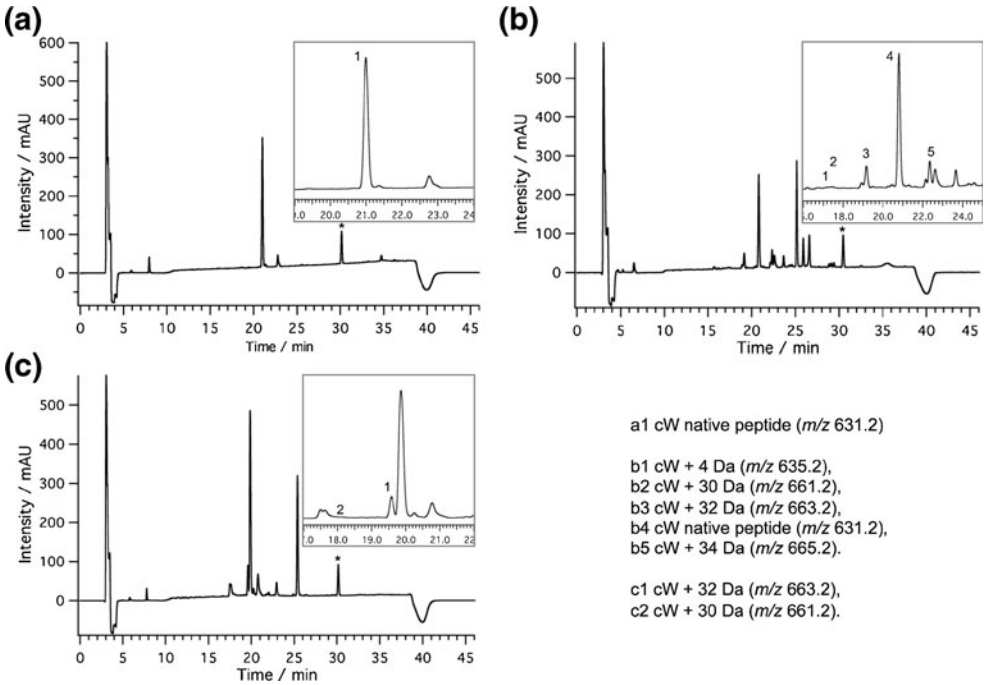

Figure 2. UV chromatograms at 214 nm of cW+UV only (**a**), amotosalen/UVA treated (**b**), and riboflavin/UVB treated (**c**). See inset and legend for peak details. Other main peaks correspond to degradation products of amotosalen or riboflavin (see Figure 1). *Contaminant coming from InterSol

and in Supporting Information); the results on oxidations are summarized in Table 2. There is a clear formation of new LC peaks at different retention times for treated samples compared with untreated ones. The native cW peptide eluted in 20.9 min (*m*/*z* 631.2) (Figure 2a, peak a1), while doubly oxidized peptide forms were visible in low amount at 17.4, 17.6, 19.2, 20.5 min (peak b1: *m*/*z* 635.2, peaks b2, c2: *m*/*z* 661.2, peaks b3, c1: *m*/*z* 663.2, peak b5: *m*/*z* 665.2, respectively, in Figure 2b and c.

These modification sites, on Trp, were identified by MS/MS and tandem mass spectra are shown in Figure 3 (probable structures are shown in inset). Fragments were recalculated according to the modification and matched with experimental data. The asterisk (*) on W stands for a cW+4/30/32 or 34 Da. Thus, the oxidations were clearly identified on the Trp moiety. As for the modification at +30 Da (b3 ion not detected and W* labeling absent), the presence of native b4 +30 Da and native y4 +30 Da ions confirms the modification on Trp. The +4 Da probably consists in a dealkylation after opening of the indole heterocycle, followed by the formation of a ketone (peak b1: *m*/*z* 635.2 in Figure 2b) [41] and the +30 Da, +32 Da in a cycle opening and aldehyde and enone or kenone formation (peaks b2, b3, and c1, c2 in Figure 2) [42, 43]. Finally, the +34 Da is expected to correspond to an addition of two hydroxyl groups, which would agree with radical reactions involved in presence of ROS (peak b5 in Figure 2). A reduction of the cW +32 Da species to form an alcohol is probably not involved under this oxidative environment [39, 52, 53].

Depending on oxidation conditions, amino acids can be modified in different manners [43]. Different oxidation sites on peptides were observed in function of amino acids and PRT (see Table 2), after inactivation treatments, and confirmed by MS/MS (see Figures S21–S34 in Supporting Information). All peptides, after exposure to UV and photosensitizers, exhibited at least one modification. cH formed two new peaks at 14.3 and 15.2 min (*m*/*z* 596.2) after treatment where His was singly oxidized (addition of one oxygen atom, see Supporting Information) [47]. The differences in retention times are due to the polarity of the species, which is explained by oxidations at different sites. The other histidine-containing peptide, angII (see Table 2 and Supporting Information), exhibited two other oxidations at +16 Da and +32 Da corresponding to single and double histidine oxidation [43, 51]. On tyrosine-containing peptides (YY, angII, and M peptides, see Table 2 and Supporting Information), three oxidations were observed (i.e. +16, +30 and +32 Da). The double oxidations (+30 and +32 Da of the unmodified peptide) are known to be located on aromatic ring and β carbon [48, 49] and suggest that keto-enol tautomerism is possible [54]. Finally, the cysteine-containing peptides (cC and Fib Seq, see Table 2 and Supporting Information) formed mainly disulfide bonds, sulfenic and sulfonic acids according to mass shift of −2 Da, +16 Da, and +48 Da of the native peptide [39, 44–46]. Cys, His, Tyr, and Trp were found to be sensitive to ROS. In fact, those units could accommodate multiple kinds of oxidations (e.g., single or double oxidation). Most of our results fit with oxidation of amino acids already listed and investigated in the literature. Only a small part of the modifications were not identified and remains unknown.

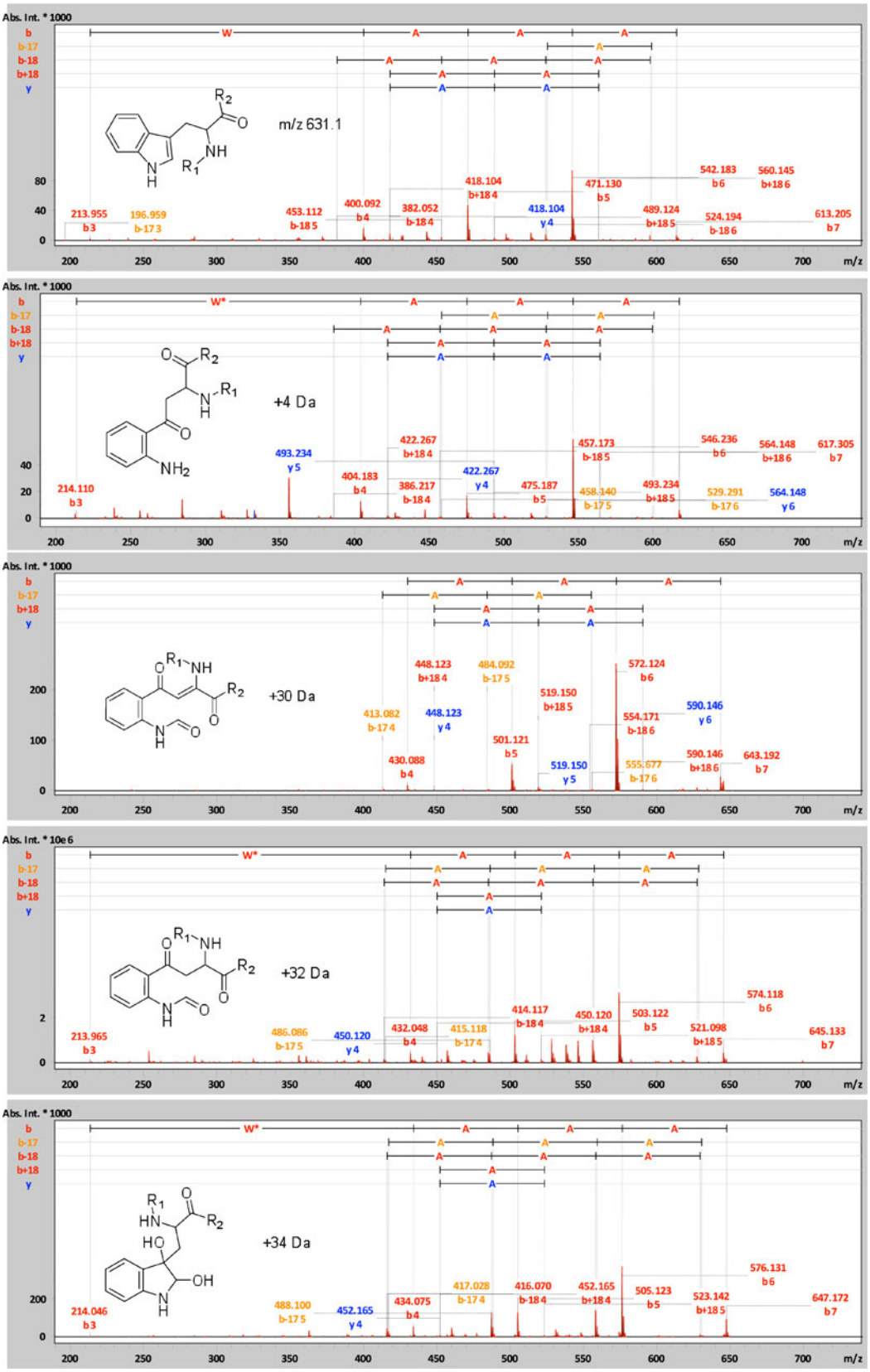

Figure 3. Tandem mass spectra of native cW peptide (*m/z* 631.3) and oxidized cW (*m/z* 631.1, +4/30/32 or 34 Da). The proposed structures were based on [41–43]. The +34 Da modification is expected to be a double addition of hydroxyl group. The MS/MS peaks were assigned to fragments using BioTools. Fragments were recalculated according to the modification and matched with experimental data. The asterisk (*) W stands for a W+4/30/32 or 34 Da

Table 2. Types and Sites of Modifications of Peptides; "y" is Set for Yes, "n" for Not Found, and "?" For Non-Identified Modification Sites

Peptide	*m/z*	Mass shift (z = 1)	Site	Oxidation type reaction	Amotosalen/UVA	Riboflavin/UVB
cC	(z = 1) 548.2 monomer	–	–	–		
	(z = 2) 547.7 dimer	–2 Da	Cys	Disulfide bond [39, 44–46]	y	y
	(z = 2) 555.7 dimer	+16 Da	Cys	Sulfenic acid [39, 45, 46]	y	n
	578.2	+30 Da	Cys	Non-identified	y	y
	596.2	+48 Da	Cys	sulfonic acid [39, 44–46]	y	y
cH	(z =1) 582.3 monomer	–	–	–		
	596.3	+14 Da	His	Ketone: formation of 2–oxo-histidine [47]	y	y
cW	(z = 1) 631.2 monomer	–	–	–		
	661.2	+30 Da	Trp	Opening cycle, aldehyde and enone formation [42]	y	y
	663.2/647.2	+32 Da/+16 Da	Trp	Opening cycle, aldehyde and ketone formation / single ox [43]	y	y
	665.2	+34 Da	Trp	Double addition of hydroxyl	y	n
	635.2	+4 Da	Trp	opening heterocycle, dealkylation and ketone formation [41]	y	n
YY	(z = 1) 345.1 monomer	–	–	–		
	375.1	+30 Da	Tyr	Double oxidation, double keton on aromatic ring and ß carbon [48]	y	y
	377.1	+32 Da	Tyr	Double oxidation, on aromatic ring and ß carbon [48, 49]	y	y
M	(z = 1) 636.2 monomer	–	–	–		
	652.2/668.2	+16 Da/+32 Da	Tyr	Single oxidation/double oxidation [48, 50]	y	y
	681.2/716.2	+45 Da/+80 Da[a]	? [a]	Non-identified	y	y
angII	(z = 2) 523.7 monomer	-	-	-		
	530.7	+14 Da	His	Single oxidation [47]	y	y
	531.8	+16 Da	His	Single oxidation [43]	y	y
	538.7	+30 Da	Tyr	Double oxidation [48]	y	y
	539.7	+32 Da	His	Double oxidation [51]	y	y
	546.7	+46 Da[b]	? [b]	Non-identified	n	y
	555.8	+64 Da[a]	? [a]	Non-identified	n	y
Fib seq.	(z = 2) 625.7 monomer	–	–	–		
	1,248.4 dimer	–2 Da	Cys	Disulfide bond [44]	y	y
	649.7	+48 Da	Cys	Sulfonic acid [44]	y	y
	(z = 3) 843.3 dimer	+32 Da[a]	Tyr[a]	Double oxidation [48]	y	y
	(z = 3) 842.6 dimer	+30 Da[a]	Tyr[a]	Double oxidation [48]	y	n

[a]MS/MS too weak or not clear enough to confirm the potential oxidation site.
[b]+32 Da confirmed on His by y2, y3, and b6 ions. Possible +14 Da on Tyr. See Supporting Information.

Quantification of modifications was performed by integrating the peak areas of the UV chromatograms to compare the two oxidative processes and the reactivity of peptides towards the photoactive molecules. The two graphs in Figure 4 show the conversion rates in percent of the oxidized species (both disulfide bridges dimer and M_{ox}) and the remaining native peptide. The seven peptides were all oxidized to different extents; in particular cC, cH, cW, and Fib seq are very sensitive to pathogen inactivation processes, as clearly shown in Figure 4a. It is interesting to note that in general, the riboflavin/UVB process generates higher amount of oxidized species. As for cysteine-containing peptides (cC and Fib seq) the oxidations are distributed between disulfide bridges and sulfenic and sulfonic acids (see Figure 5). Even though there is no difference between the two treatments on both types of oxidation, the data are statistically different for cC (same trend observed for Fib seq) when considering dimer and M_{ox} separately. Comparing controls (i.e., peptide + UV only) with treated samples, the inactivation processes forced dimer and oxidized species formation, totally consuming the monomer form in the case of Fib seq peptide. In both cases, higher oxidation levels were observed compared with control and the irreversible sulfonic acid form (i.e., shift of +48 Da, R-SO_3H) was more abundant with riboflavin/UVB, whereas dimerization was higher with amotosalen/UVA.

A general tendency was clearly observed with a major oxidation rate for riboflavin/UVB treated peptides. Riboflavin/UVB is a very powerful oxidizing process for tryptophan, histidine, and tyrosine (see Figure 4). In contrast, cysteine-containing peptides and angII do not present any important differences compared with the other five peptides.

As a final remark, photoadducts were not observed either on Tyr or on other residues. Post-analyses using extracted ion chromatograms of possible adduct formation were applied and no modification could be found. However, it is not excluded that the very low abundance of such modifi-

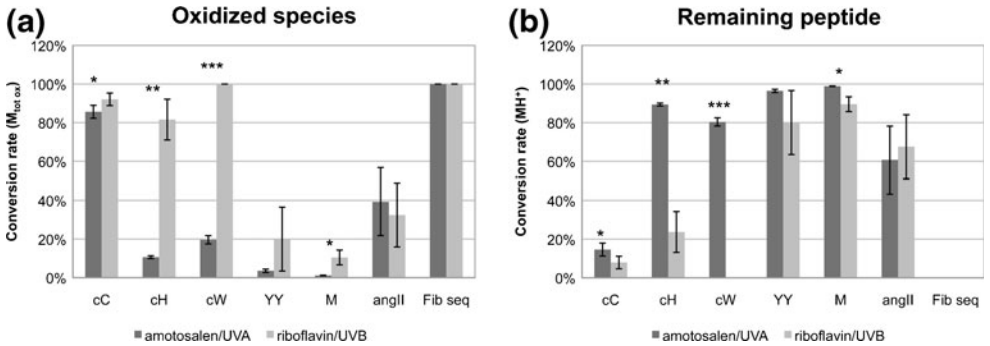

Figure 4. (**a**) Level of peptide oxidation (both disulfide bridges dimer and oxidation M_{ox}, see Equation 3) after treatment. (**b**) Percent of unmodified peptide after treatments. Riboflavin/UVB highlights higher conversion rates than amotosalen/UVA. Oxidation of cysteine-containing peptides are detailed in Figure 5. $^{*}P<0.05$, $^{**}P<0.01$, $^{***}P<0.001$ ($n = 3$)

cations (a few adducts per thousand of amino acids [36]) renders difficult any detection of adducts with our analytical setup.

Discussion

The results presented here show that the photochemical treatments, used to inactivate pathogens in PC, induce the oxidation of peptides to different extents depending on the peptide composition and the PRT. The concentration of the photosensitizers, amotosalen and riboflavin, were 100 µM, which slightly differs from the one used in routinely (i.e., 150 µM of amotosalen in amotosalen/UVA and 50 µM of riboflavin in riboflavin/UVB). It was a compromise in order to compare their reactivity with a ratio photosensitizer/peptide of 2. Even though the concentration of photosensitizers is close to the one used routinely, the ratio is different from the one in PC. Indeed, the model peptides were exposed to an excess of amotosalen or riboflavin, whereas the ratio in PC is around 0.1 (approximately 80 g/L of plasma and platelet proteins per PC, considering mainly albumin) and 0.04, for Intercept and Mirasol, respectively. In PC, the targets are primary nucleic acids, and potentially other proteins and other metabolites, whereas under our conditions the targets for oxidation are the peptide and the photosensitizer itself. However, these experiments were designed in view of highlighting the potential sites and types of modifications occurring on peptides and to compare both amotosalen/UVA and riboflavin/UVB treatments at the peptide level.

Cysteine-containing peptides (cC and Fib seq) exhibited the formation of disulfide bridges and sulfonic acids. Both types of oxidation are present before the photochemical treatment (except the sulfonic acid form of cC) and were not influenced by UV treatment alone. This phenomenon cannot only be explained by the oxidation of the free cysteine by oxidants already present in solution but also by the analysis itself known for its oxidative properties [39, 52, 53]. The two peptides were affected differently by the treatments as shown by the formation of dimers (see Figure 5). Dimers are more important with amotosalen/UVA than with riboflavin/UVB, whereas the oxidation, M_{ox}, is more pronounced with

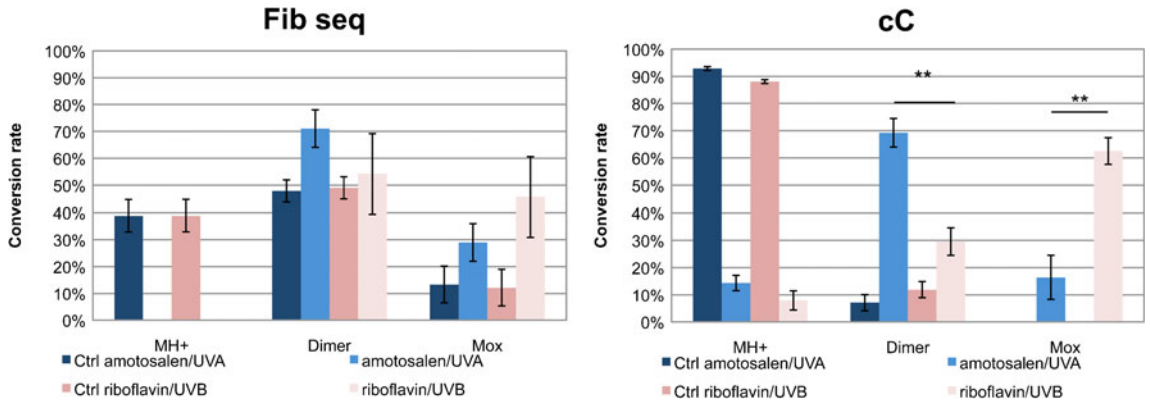

Figure 5. Detailed conversion rates of cysteine-containing peptides calculated according to Equations 1 and 2. Along the x-axis: monomer (z = 1) MH^+, the dimer (z = 1 and z = 2), and the oxidized species M_{ox} are represented. cC: dimer form is already present in the untreated peptide. Fib seq: dimer and the +48 Da oxidation (sulfonic acid) forms are already present in the untreated peptide. Ctrl: peptides+UV only. $^{**}P<0.01$ ($n = 3$)

riboflavin/UVB. It can be explained by the type of mechanism involved, where a type I might be favored in amotosalen/UVA treatment.

The oxidation rate observed with the other peptides (cH, cW, YY, M, and angII) is peptide- and amino acid-dependent, and is as follows: Trp>His>Tyr-containing peptides, which is more or less in agreement with the literature for the quenching of $^1O_2$ [32, 33]. The tyrosine seems to be less affected (see Figure 4), which pleads in favor of type II mechanism that involves $^1O_2$. Indeed, Tyr residues react faster than the other amino-acids, under a type I mechanism (through psoralen radicals) [34] than under type II [32].

Moreover, the sequence influences the conversion rate. cC and Fib seq peptides, both containing cysteine residues, or M, YY, and angII, both containing tyrosine and/or histidine residues, have different reactivities. By extension, proteins from the platelet and residual plasma may behave differently upon PRT treatments and the oxidation level will be influenced by the tertiary structure.

The oxidation power of the two PRT tested here is different and, under these conditions, the riboflavin/UVB induces more oxidation than amotosalen/UVA (see Figure 4). Even though the impact on PRT is not straightforward and that these data need to be kept under this context of peptide oxidation, it indicates that these processes act differently, as highlighted by the cysteine-containing peptides and the type of photochemical processes involved, for instance, and may differently impact the platelet and plasma proteins. Platelet proteomic analyses have revealed that Intercept and Mirasol do not impact the same proteins, and that Mirasol tends to affect more the cytoskeleton organization and platelet shape change than Intercept [24]. Even though they reported some oxidative stress, these studies do not probe the reactivity of disulfide bridges (proteins are reduced during the different workflows) and do not directly focus on redox-proteomics. Other approaches will be required to look at the impact of PRT on protein oxidative damages, and they could reveal more oxidation. All these oxidative damages can alter the structure and the function of proteins and, thus, the platelet function and the aggregation properties in hemostasis, as shown by the oxidation of the fibronectin sequence (a collagen binding fragment) that is involved in thrombus formation [37].

Conclusions

The present data clearly highlight the possible targets and types of modifications on peptides, which will allow us to probe modifications at the protein level. Moreover, the two phototreatments of PC behave differently on peptide oxidations. Even though they induce oxidations of amino acids side chains and the formation of disulfide bridges in cysteine-containing peptides, the rates of oxidation are different. The impact on the proteins and platelet functions may thus be different in the case of the riboflavin-based PRT that acts by generating ROS only. These results will help in understanding the damages at the protein level studies that are currently under investigation in our laboratory.

PRT are progressively introduced in several countries and agencies that approved the systems need to base their decisions on several studies. Proteomics and in vitro studies have already revealed the potential impacts. Here, the picture is enriched by the oxidative effects related to PRT. Further redox-proteomic approaches will have to be tested in order to pursue these analyses at the protein level.

Acknowledgments

The authors thank the Commission de Recherche du Service de Transfusion Sanguine de la Croix-Rouge suisse for financial support. Mr. Guillaume Riat and Mr. David Crettaz are thanked for their help in building the homemade setup.

References

1. Irsch, J., Lin, L.: Pathogen inactivation of platelet and plasma blood components for transfusion using the INTERCEPT blood system (TM). Transfus. Med. Hemother. **38**, 19–31 (2011)
2. Marschner, S., Goodrich, R.: Pathogen reduction technology treatment of platelets, plasma and whole blood using riboflavin and UV light. Transfus. Med. Hemother. **38**, 8–18 (2011)
3. Available at: http://www.aabb.org/resources/bct/eid/Documents/prt-systems-in-routine-use-country-listing.pdf. Accessed 10 April 2013
4. Cazenave, J.P., Follea, G., Bardiaux, L., Boiron, J.M., Lafeuillade, B., Debost, M., Lioure, B., Harousseau, J.L., Tabrizi, R., Cahn, J.Y., Michallet, M., Ambruso, D., Schots, R., Tissot, J.D., Sensebe, L., Kondo, T., McCullough, J., Rebulla, P., Escolar, G., Mintz, P., Heddle, N.M., Goodrich, R.P., Bruhwyler, J., Le, C., Cook, R.J., Stouch, B.: Mirasol Clinical Evaluation, S.: A randomized controlled clinical trial evaluating the performance and safety of platelets treated with MIRASOL pathogen reduction technology. Transfusion **50**, 2362–2375 (2010)
5. Janetzko, K., Cazenave, J.P., Kluter, H., Kientz, D., Michel, M., Beris, P., Lioure, B., Hastka, J., Marblie, S., Mayaudon, V., Lin, L., Lin, J.S., Conlan, M.G., Flament, J.: Therapeutic efficacy and safety of photochemically treated apheresis platelets processed with an optimized integrated set. Transfusion **45**, 1443–1452 (2005)
6. Lozano, M., Knutson, F., Tardivel, R., Cid, J., Maymo, R.M., Lof, H., Roddie, H., Pelly, J., Docherty, A., Sherman, C., Lin, L., Propst, M., Corash, L., Prowse, C.: A multi-centre study of therapeutic efficacy and safety of platelet components treated with amotosalen and ultraviolet A pathogen inactivation stored for 6 or 7 days prior to transfusion. Br. J. Haematol. **153**, 393–401 (2011)
7. van Rhenen, D., Gulliksson, H., Cazenave, J.P., Pamphilon, D., Ljungman, P., Kluter, H., Vermeij, H., Kappers-Klunne, M., de Greef, G., Laforet, M., Lioure, B., Davis, K., Marblie, S., Mayaudon, V., Flament, J., Conlan, M., Lin, L., Metzel, P., Buchholz, B., Corash, L.: Transfusion of pooled buffy coat platelet components prepared with photochemical pathogen inactivation treatment: the euroSPRITE trial. Blood **101**, 2426–2433 (2003)
8. Infanti, L., Stebler, C., Job, S., Ruesch, M., Gratwohl, A., Irsch, J., Lin, L., Buser, A.: Pathogen-inactivation of platelet components with the INTERCEPT blood system (TM): A cohort study. Transfus. Apher. Sci. **45**, 175–181 (2011)
9. Corash, L., Sherman, C.D.: Evaluation of platelet transfusion clinical trials. Br. J. Haematol. **153**, 529–531 (2011)
10. Kerkhoffs, J.L.H.: Evaluation of platelet transfusion clinical trials - response to Corash & Sherman. Br. J. Haematol. **153**, 531–532 (2011)
11. Kerkhoffs, J.L.H., van Putten, W.L.J., Novotny, V.M.J., Boekhorst, P., Schipperus, M.R., Zwaginga, J.J., van Pampus, L.C.M., de Greef, G.E., Luten, M., Huijgens, P.C., Brand, A., van Rhenen, D.J., Dutch Belgian, H.C.G.: Clinical effectiveness of leucoreduced, pooled donor platelet

concentrates, stored in plasma or additive solution with and without pathogen reduction. Br. J. Haematol. **150**, 209–217 (2010)
12. Sigle, J.-P., Infanti, L., Studt, J.-D., Martinez, M., Stern, M., Gratwohl, A., Passweg, J., Tichelli, A., Buser, A.S.: Comparison of transfusion efficacy of amotosalen-based pathogen-reduced platelet components and gamma-irradiated platelet components. Transfusion **53**, 1788–1797 (2013)
13. Apelseth, T.O., Bruserud, O., Wentzel-Larsen, T., Bakken, A.M., Bjorsvik, S., Hervig, T.: In vitro evaluation of metabolic changes and residual platelet responsiveness in photochemical treated and gamma-irradiated single-donor platelet concentrates during long-term storage. Transfusion **47**, 653–665 (2007)
14. Hechler, B., Ohlmann, P., Chafey, P., Ravanat, C., Eckly, A., Maurer, E., Mangin, P., Isola, H., Cazenave, J.-P., Gachet, C.: Preserved functional and biochemical characteristics of platelet components prepared with amotosalen and ultraviolet A for pathogen inactivation. Transfusion **53**, 1187–1200 (2013)
15. Goodrich, R.P., Li, J.Z., Pieters, H., Crookes, R., Roodt, J., Heyns, A.D.: Correlation of in vitro platelet quality measurements with in vivo platelet viability in human subjects. Vox Sang. **90**, 279–285 (2006)
16. Perez-Pujol, S., Tonda, R., Lozano, M., Fuste, B., Lopez-Vilchez, I., Galan, A.M., Li, J., Goodrich, R., Escolar, G.: Effects of a new pathogen-reduction technology (Mirasol PRT) on functional aspects of platelet concentrates. Transfusion **45**, 911–919 (2005)
17. Picker, S.M., Tauszig, M.E., Gathof, B.S.: Cell quality of apheresis-derived platelets treated with riboflavin-ultraviolet light after resuspension in platelet additive solution. Transfusion **52**, 510–516 (2012)
18. Marrocco, C., D'Alessandro, A., Girelli, G., Zolla, L.: Proteomic analysis of platelets treated with gamma irradiation versus a commercial photochemical pathogen reduction technology. Transfusion **53**, 1808–1820 (2013)
19. Prudent, M., Crettaz, D., Delobel, J., Tissot, J.-D., Lion, N.: Proteomic analysis of Intercept-treated platelets. J. Proteom. **76**, 316–328 (2012)
20. Schubert, P., Culibrk, B., Coupland, D., Scammell, K., Gyongyossy-Issa, M., Devine, D.V.: Riboflavin and ultraviolet light treatment potentiates vasodilator-stimulated phosphoprotein Ser-239 phosphorylation in platelet concentrates during storage. Transfusion **52**, 397–408 (2012)
21. Thiele, T., Iuga, C., Janetzky, S., Schwertz, H., Gesell Salazar, M., Furll, B., Volker, U., Greinacher, A., Steil, L.: Early storage lesions in apheresis platelets are induced by the activation of the integrin alphaIIbbeta(3) and focal adhesion signaling pathways. J Proteom **76**, 297–315 (2012)
22. Thiele, T., Sablewski, A., Iuga, C., Bakchoul, T., Bente, A., Gorg, S., Volker, U., Greinacher, A., Steil, L.: Profiling alterations in platelets induced by Amotosalen/UVA pathogen reduction and gamma irradiation—a LC-ESI-MS/MS-based proteomics approach. Blood Transf. **10**, S63–S70 (2012)
23. Prudent, M., Tissot, J.D., Lion, N.: Proteomics of blood and derived products: What's next? Exp. Rev. Proteom. **8**, 717–737 (2011)
24. Prudent, M., D'alessandro, A., Cazenave, J.P., Devine, D.V., Gachet, C., Greinacher, A., Lion, N., Schubert, P., Steil, S., Thiele, T., Tissot, J.-D., Völker, U., Zolla, L.: Proteome changes in platelets after pathogen inactivation – an interlaboratory consensus, submitted
25. Cao, H.C., Hearst, J.E., Corash, L., Wang, Y.S.: LC-MS/MS for the detection of DNA interstrand cross-links formed by 8-methoxypsoralen and UVA irradiation in human cells. Anal. Chem. **80**, 2932–2938 (2008)
26. Lai, C.F., Cao, H.C., Hearst, J.E., Corash, L., Luo, H., Wang, Y.S.: Quantitative analysis of DNA interstrand cross-links and monoadducts formed in human cells induced by psoralens and UVA irradiation. Anal. Chem. **80**, 8790–8798 (2008)
27. Caffieri, S.: Furocoumarin photolysis: chemical and biological aspects. Photochem. Photobiol. Sci. **1**, 149–157 (2002)
28. Kitamura, N., Kohtani, S., Nakagaki, R.: Molecular aspects of furocoumarin reactions: photophysics, photochemistry, photobiology, and structural analysis. J. Photochem. Photobiol. C-Photochem. Rev. **6**, 168–185 (2005)
29. Averbeck, D., Moustacchi, E., Bisagni, E.: Biological effects and repair of damage photoinduced by a derivative of psoralen substituted at 3,4 reaction site—photoreactivity this compound and lethal effect in, yeast. Biochimica et Biophysica Acta **518**, 464–481 (1978)
30. Cardoso, D.R., Libardi, S.H., Skibsted, L.H.: Riboflavin as a photosensitizer. Effects on human health and food quality. Food Funct. **3**, 487–502 (2012)
31. Barelli, S., Canellini, G., Thadikkaran, L., Crettaz, D., Quadroni, M., Rossier, J.S., Tissot, J.D., Lion, N.: Oxidation of proteins: basic principles and perspectives for blood proteomics. Proteom. Clin. Appl. **2**, 142–157 (2008)
32. Remucal, C.K., McNeill, K.: Photosensitized amino acid degradation in the presence of riboflavin and its derivatives. Environ. Sci. Technol. **45**, 5230–5237 (2011)
33. Rougee, M., Bensasson, R.V., Land, E.J., Pariente, R.: Deactivation of singlet molecular-oxygen by thiols and related-compounds, possible protectors against skin photosensitivity. Photochem. Photobiol. **47**, 485–489 (1988)
34. Wood, P.D., Mnyusiwalla, A., Chen, L., Johnston, L.J.: Reactions of psoralen radical cations with biological substrates. Photochem. Photobiol. **72**, 155–162 (2000)
35. Sastry, S.S.: Isolation and partial characterization of a novel psoralen-tyrosine photoconjugate from a photoreaction of psoralen with a natural protein. Photochem. Photobiol. **65**, 937–944 (1997)
36. Schmitt, I.M., Chimenti, S., Gasparro, F.P.: Psoralen protein photochemistry—a forgotten field. J. Photochem. Photobiol. B-Biol. **27**, 101–107 (1995)
37. Cho, J., Mosher, D.F.: Role of fibronectin assembly in platelet thrombus formation. J. Thromb. Haemost. **4**, 1461–1469 (2006)
38. Hardwick, C.C., Herivel, T.R., Hernandez, S.C., Ruane, P.H., Goodrich, R.P.: Separation, identification, and quantification of riboflavin and its photoproducts in blood products using high-performance liquid chromatography with fluorescence detection: a method to support pathogen reduction technology. Photochem. Photobiol. **80**, 609–615 (2004)
39. Prudent, M., Girault, H.H.: The role of copper in cysteine oxidation: study of intra- and intermolecular reactions in mass spectrometry. Metallomics **1**, 157–165 (2009)
40. Liu, W.Q., Cimino, G.D., Corash, L., Lin, L.L.: The extent of amotosalen photodegradation during photochemical treatment of platelet components correlates with the level of pathogen inactivation. Transfusion **51**, 52–61 (2011)
41. Todorovski, T., Fedorova, M., Hoffmann, R.: Mass spectrometric characterization of peptides containing different oxidized tryptophan residues. J. Mass Spectrom. **46**, 1030–1038 (2011)
42. Domingues, M.R.M., Domingues, P., Reis, A., Fonseca, C., Amado, F.M.L., Ferrer-Correia, A.J.V.: Identification of oxidation products and free radicals of tryptophan by mass spectrometry. J. Am. Soc. Mass Spectrom. **14**, 406–416 (2003)
43. Ji, J.A., Zhang, B., Cheng, W., Wang, Y.J.: Methionine, tryptophan, and histidine oxidation in a model protein, PTH: mechanisms and stabilization. J. Pharm. Sci. **98**, 4485–4500 (2009)
44. Chang, Y.-C., Huang, C.-N., Lin, C.-H., Chang, H.-C., Wu, C.-C.: Mapping protein cysteine sulfonic acid modifications with specific enrichment and mass spectrometry: an integrated approach to explore the cysteine oxidation. Proteomics **10**, 2961–2971 (2010)
45. Men, L., Wang, Y.S.: Further studies on the fragmentation of protonated ions of peptides containing aspartic acid, glutamic acid, cysteine sulfinic acid, and cysteine sulfonic acid. Rapid Commun. Mass Spectrom. **19**, 23–30 (2005)
46. Tsaprailis, G., Nair, H., Somogyi, A., Wysocki, V.H., Zhong, W.Q., Futrell, J.H., Summerfield, S.G., Gaskell, S.J.: Influence of secondary structure on the fragmentation of protonated peptides. J. Am. Chem. Soc. **121**, 5142–5154 (1999)
47. Schöneich, C.: Mechanisms of metal-catalyzed oxidation of histidine to 2-oxo-histidine in peptides and proteins. J. Pharmaceut. Biomed. **21**, 1093–1097 (2000)
48. Fonseca, C., Domingues, M.R.M., Simões, C., Amado, F., Domingues, P.: Reactivity of Tyr–Leu and Leu-Tyr dipeptides: identification of oxidation products by liquid chromatography-tandem mass spectrometry. J. Mass Spectrom. **44**, 681–693 (2009)
49. Wright, A., Bubb, W.A., Hawkins, C.L., Davies, M.J.: Singlet oxygen-mediated protein oxidation: evidence for the formation of reactive side chain peroxides on tyrosine residues. Photochem. Photobiol. **76**, 35–46 (2002)

50. Surwase, S.N., Jadhav, J.P.: Bioconversion of L-tyrosine to L-DOPA by a novel bacterium Bacillus sp. JPJ. Amino Acids **41**, 495–506 (2011)
51. Gracanin, M., Hawkins, C.L., Pattison, D.I., Davies, M.J.: Singlet-oxygen-mediated amino acid and protein oxidation: formation of tryptophan peroxides and decomposition products. Free Rad. Biomed. **47**, 92–102 (2009)
52. Prudent, M., Girault, H.H.: Functional electrospray emitters. Analyst **134**, 2189–2203 (2009)
53. Van Berkel, G.J., Kertesz, V.: Using the electrochemistry of the electrospray ion source. Anal. Chem. **79**, 5510–5520 (2007)
54. Iglesias, E.: Tautomerization of 2-acetylcyclohexanone. 1. Characterization of keto−enol/enolate equilibria and reaction rates in water. J. Org. Chem. **68**, 2680–2688 (2003)